Ecotoxicology and Environmental Safety 133 (2016) 10–17

Contents lists available at ScienceDirect

Ecotoxicology and Environmental Safety

journal homepage: www.elsevier.com/locate/ecoenv

Antioxidant enzyme activities as biomarkers of fluvial biofilm to ZnO NPs ecotoxicity and the Integrated Biomarker Responses (IBR) assessment

Jun Hou [a,b], Guoxiang You [a,b], Yi Xu [a,b], Chao Wang [a,b], Peifang Wang [a,b,*], Lingzhan Miao [a,b], Shanshan Dai [a,b], Bowen Lv [a,b], Yangyang Yang [a,b]

[a] Key Laboratory of Integrated Regulation and Resources Development on Shallow Lakes, Ministry of Education, Hohai University, Nanjing 210098, People's Republic of China
[b] College of Environment, Hohai University, Nanjing 210098, People's Republic of China

ARTICLE INFO

Article history:
Received 28 March 2016
Received in revised form
8 June 2016
Accepted 10 June 2016
Available online 8 July 2016

Keywords:
Antioxidant enzymes activities
Fluvial biofilm
ZnO NPs
Integrated Biomarker Responses

ABSTRACT

The presence of ZnO nanoparticles (ZnO NPs) in natural waters has raised concerns about their environmental impacts, but the potential influences of ZnO NPs on fluvial biofilm have not been reported. In this study, the utility of antioxidant enzyme activities (AEA) as biomarkers of fluvial biofilm to ZnO NPs toxicity and a method that combines AEA into an index of "Integrated Biomarker Responses (IBR)" were studied. Compared with the absence of ZnO NPs, scanning electron microscopy (SEM) images revealed that a large amount of ZnO NPs were adsorbed onto biofilm and these NPs exerted adverse effects on the viability of bacteria in biofilm. The production of reactive oxygen species (ROS) with high concentrations (30 and 100 mg/L) of ZnO NPs exposure reached to 184% and 244% of the control, while no cell leakage and membrane damage were observed. After exposure to ZnO NPs for 0.25 and 3 days, the activities of catalase (CAT), superoxide dismutase (SOD) and glutathione reductase (GR), glutathione peroxidase (GSH-Px) were significantly increased, respectively. At the end of exposure period (21 days), the AEA with the presence of 1 mg/L ZnO NPs exposure were comparable to the control, while most of those in high concentrations of ZnO NPs were decreased. The results of IBR showed that the biofilm can adapt to 1 mg/L ZnO NPs exposure, while be seriously damaged by 30 and 100 mg/L ZnO NPs after 3 and 0.25 days. IBR can be used as an appropriate evaluation system of the toxicity effects of ZnO NPs on fluvial biofim.

1. Introduction

As an emerging industry, nanotechnology have drawn much attention because of the unique optics properties, catalytic capacity and antimicrobial activity of nanoparticles (NPs) (Roco, 2005; Maynard et al., 2006). These characteristics make them attractive for a wide range of applications (Ma et al., 2013) in industrial, medical and military (Serda et al., 2009). With the world wide utilization of these nano-products, it is inevitable for the release of increasing quantities of NPs from existed source to environment receptors (Brar et al., 2010), such as atmospheric air, soil and water bodies (Nowack and Bucheli, 2007; Hendren et al., 2011). It is therefore necessary to evaluate their influences on the environment.

ZnO NPs, one of the most interest metal oxide NPs, due to their unique physical and chemical properties, including pyroelectric, piezoelectric and biocompatible properties (Wang and Song, 2006; Zhu et al., 2007), have been widely used in semiconductors, plastic additives, pigments and cosmetics (Zheng et al., 2011). Nevertheless, research about the antimicrobial activity of ZnO NPs showed that once ZnO NPs are released into the environment, they could be adsorbed and exert diverse negative effects on the exposed algae, pure culture microorganism and activated sludge (Boxall et al., 2007; Zheng et al., 2011; Suman et al., 2015), including changing the diversity and composition of bacterial communities, reducing the activities of bacteria and damaging the structure of deoxyribonucleic acid (DNA) in cells (Ma et al., 2013). In addition, oxidative stress of ZnO NPs has also been observed in previous study, due to its capacity to enhance the production of reactive oxygen species (ROS) (Zheng et al., 2011). Although the occurrence and implication of ZnO NPs on biofilms and activated sludge in wastewater treatment plants have recently become a mater of concern, and some ecotoxicological effects have also been revealed (Hou et al., 2014), the effects of ZnO-NPs on biofilms in natural waters and the related mechanisms remain unknown.

* Correspondence to: College of Environment, Hohai University, 1 Xikang Road, Nanjing 210098, People's Republic of China.
E-mail address: pfwang2005@hhu.edu.cn (P. Wang).

http://dx.doi.org/10.1016/j.ecoenv.2016.06.014
0147-6513/

Biofilms in natural water are also known as periphyton and phytobenthos, which consist of diverse microorganisms, such as algae, bacteria, fungi and protozoa, that embed in the extracellular matrices of polymeric substances (Flemming and Wingender, 2010). With the fixation abilities of extracellular polymeric substances (EPS) and the high biomass, biofilms have been extensively applied in water bodies or wastewater treatment plants to degrade contaminants (Battin et al., 2003). Biosorption is considered to be the major physical removal mechanism for pollutants, leading to accumulation of these compounds in biofilms (Kiser et al., 2010). Moreover, some studies (Zheng et al., 2011; Hou et al., 2014) have confirmed that the antimicrobial activity of ZnO NPs could inhibit the microbial activity in the outer biofilm layer and activated sludge, thus decrease the biological nitrogen and phosphorus removal efficiency in wastewater treatment plants. However, knowledge about the responses of biofilms in natural waters exposed to ZnO-NPs is unavailable.

Research on the responses of wastewater biofilms and activated sludge to NPs exposure have suggested that most NPs can produce several toxic effects, which are mainly thought to be caused by the enhancement of ROS in bacteria (Hou et al., 2014, 2015a). Studies demonstrated that ZnO NPs may accelerate an increase in ROS production in autotrophic organism and lead to the oxidative stress in cells (Cuypers et al., 2001; Zheng et al., 2011). As a defense system, the antioxidant enzyme activities (AEA), such as catalase (CAT), glutathione reductase (GR), superoxide dismutase (SOD) and glutathione peroxidase (GSH-Px), play an important part in maintaining the degree of ROS and defensing the oxidative stress that results from the toxic pollutants (Collén et al., 2003; Valavanidis et al., 2006). While most AEA studies have been conducted on pure strains (Tripathi et al., 2006), with less frequency in microflora systems, which contain a various complex communities, followed by offering a poor and lower standard of ecological realism (Clements and Newman, 2002; Bonet et al., 2012). Previous studies tend to choose AEA as the sensitive indicator for pollution caused by metal ions (i.e. Zn^{2+} and Cu^{2+}) (Valavanidis et al., 2006; Bonet et al., 2014), while no studies were conducted to evaluate the pollution levels of NPs in biofilms with AEA. Therefore, there is an urgent need to understand the defense mechanisms and responses of AEA in fluvial biofilms after exposure to ZnO NPs. Additionally, Bonet et al. (2014) have shown that the response of AEA to stress is usually not liner and is more likely to change with chronic exposure by reason of adaptation. Bonnineau (2011) also claimed that AEA follow a unimodal pattern with various patterns of activity: increase, decrease, inhibition and saturation. Thus the application of AEA is limited unless they are integrated into a general scheme facilitating data analysis and interpretation (Brooks et al., 2015). Integrated Biomarker Response (IBR) index, which summarizes the amount of available biomarkers in a multivariate data can afford an integrated view of the toxicity effects of pollutions (Kim et al., 2010). This approach has been widely applied in many fields and laboratory environmental risk assessment studies (Kim et al., 2010; Li et al., 2011; Serafim et al., 2012), while studies using this approach for simplifying the interpretation of biomarker responses have never been verified previously in fluvial biofilms.

The aim of this study is to investigate the ecotoxicological responses of fluvial biofilms to ZnO NPs exposure and the integrated assessment of stress level caused by ZnO NPs, by detailing the following factors:

1. To characterize the toxicity effects of ZnO NPs on fluvial biofilms and the potential toxicity mechanisms, the bacteria viability as well as standard ROS and lactate dehydrogenase (LDH) activities were analyzed in the fluvial biofilms.
2. To determine the response of biofilms in natural waters to ZnO NPs exposure, AEA were used as biomarkers (CAT, GR, SOD and GSH-Px).
3. To intuitively evaluate the stress level of ZnO NPs on fluvial biofilms, IBR was calculated and discussed.

2. Materials and methods

2.1. Nanoparticles

Commercial bare ZnO NPs (purity: $>99\%$) used in the present study were purchased as a powder (Sigma-Aldrich, St. Louis, MO) and the particle size ranged from 40 to 50 nm. The specific surface area (SSA) of ZnO NPs powder was measured to be 52.2 ± 3.5 m^2/g, via a Micromeritics Tristar 3000 analyzer by nitrogen adsorption at 77 K using the Brunauer-Emmett-Teller (BET) method. A scanning electron microscopy (SEM) image of the ZnO NPs powder was obtained using a Hitachi S-4800 SEM to visually inspect their shape (Fig. A.1, Supplementary material). Stock suspension (1 g/L) was prepared by adding 1 g of ZnO-NPs to 1 L of Milli-Q water, followed by ultrasonicating for 1 h (20 °C, 250 W, 40 kHz) (Hou et al., 2014) to break aggregates before being diluted to the exposure concentrations. The exposure medium (pH 7.4, by adding 4 M NaOH or 4 M HCl) was prepared by mixing the nutrient solution (named as S1, in Table A.1) that modified from Le Faucheur et al. (2005) with stock suspension to achieve final ZnO NPs concentrations of 1, 30 and 100 mg/L. The lowest level, 1 mg/L, was chosen as the environmentally relevant low concentration of ZnO NPs (Zheng et al., 2011). Nevertheless, considering the rapid development and growth in NPs use, 30 and 100 mg/L ZnO NPs were also examined (Adams et al., 2006). The average diameter and zeta potential of the ZnO-NPs of different concentrations in the exposure suspension were measured with a Malvern Zetasizer Nano ZS90 (Malvern Instruments, UK).

2.2. Microcosm setup and experimental design

Prior to the experiment, spherical bio-carriers with the diameter and specific surface area of 80 mm and 800 m^2/m^3 that made of polyethylene, were suspended in a natural body of water (Jiangjia River, Yixing, China) to act as carriers for microorganism attachment. The content of Zn in this river was 13–15 μg/L, and the other main parameters of this body of water are listed in Table A.2 (in Supplementary material). After 3 weeks culturing, the fillers were recaptured and suspended in the indoor microcosm system under controlled conditions, consisting of 4 recirculating channels (220 cm long, 25 cm wide and 50 cm high, details are shown in Fig. A.2, Supplementary material) to simulate nature water in laboratory. Water from the channels was replaced each day and the final nutrients concentration were listed in Table A.1, with predetermined concentrations of chemical oxygen demand 35 mg/L, total nitrogen 6 mg/L and total phosphorus 0.2 mg/L. Light was provided by halogen lamps (90–110 μmol m^{-2} s^{-1}) with a 12 h light/12 h dark cycle and the temperature was kept stable at 21 ± 1 °C. During the first four weeks of cultivation, fluvial biofilm from aliquots of bio-carriers obtained from Jiangjia River were scraped and provided weekly to each channel.

After four weeks of colonization in laboratory, a single spherical biocarrier was removed from each channel, and then the biofilm was scraped, centrifuged and dried to constant weight at 103 °C. Thereafter the dry biomass was weighed in room temperature. After observing for about one week, the dry biomass on each biocarrier was stable and the exposure experiment was started. Twelve beakers with a working volume of 2 L were used to accommodate the 0 (control), 1, 30 and 100 mg/L ZnO NPs exposure medium (each in triplicate) and mature biofilms on the carrier.

During the exposure experiment, the static displacement method modified from Hua et al. (2012) was applied to ensure the thriving growth of biofilm in the beakers. Sampling was established 6 and 3 days prior to the exposure, just before the addition of exposure medium, and after 6 h, 1, 3, 7 and 21 days; these samples were marked as −6, −3, 0, 0.25, 1, 3, 7, and 21 days, respectively.

2.3. Scanning electron microscope (SEM) with energy dispersive spectrometer (EDS)

The surface morphology of fluvial biofilms exposed to different concentrations of ZnO NPs was observed by SEM and the elements based composition adsorbed on the biofilm surface were obtained by the EDS profile. At the end of the exposure period, the biofilm samples on the carrier were scraped out. After being washed three times with 0.1 M phosphate buffer (pH 7.4), the centrifuged pellets were dehydrated in the ethanol serials (50%, 70%, 80%, 90% and 100%, 15 min per step), followed by drying in the air (Zheng et al., 2011). Finally, the SEM images were obtained by SEM (Hitachi S-4800) at 3.0 kV.

2.4. Measurements of ROS production

The intracellular ROS production in fluvial biofilms at the end of the exposure period was measured by an established fluorescence assay (Limbach et al., 2007). Biofilm samples was centrifuged at 1000 × *g* for 5 min and washed with 0.1 M phosphate buffer (pH 7.4) for 3 times. The collected pellets were then re-suspended in 0.1 M phosphate buffer containing 50 μM of dichlorodihydrofluorescein diacetate (H_2DCF-DA, Molecular Probes, Invitrogen) and incubated at 20 °C for 30 min. After the incubation, centrifugation was conducted to remove the phosphate buffer containing H_2DCF-DA. The pellets were re-suspended in exposure medium (pH 7.4) and the mixed liquor was plated into a 96-well plate. The generated fluoresce in DCF was determined after 4.5 h with a microplate reader (Biotek, USA), at excitation/emission wavelengths of 495/525 nm.

2.5. Antioxidant enzyme activities (AEA)

After −6, −3, 0, 0.25, 1, 3, 7, and 21 days of exposure, biofilms were scraped and collected from each carrier, followed by centrifugation at 4000 *g* for 10 min. Before each enzyme activity assessment, 0.5 g of wet biofilm pellets was weighted and grinded mechanically in the ice-water. During the process of grinding, 4.5 mL of saline was added to obtain the uniform suspension of cells and the suspension was centrifuged for 20 min (10,000 *g*) at 4 °C. The protein contents of the supernatant was examined by the corrected Lowry method (Li and Yang, 2007), with bovine serum albumin as a standard. The activity of CAT was measured by the reaction of the enzyme with methanol in the presence of H_2O_2 (Lars et al., 1988) and SOD activity was determined according to the method of Aebi (1984). GSH-Px activity was assayed according to Mohandas et al. (1984) and GR activity was measured as the decrease in NADH concentration (Park et al., 2008). All the chemicals were reagent grade and provided by Jiancheng Bioengineering Co. Ltd. (Nanjing, China).

2.6. Calculation of the IBR

To address the biomarkers (the AEA in this study) as a whole, a general stress index termed the "Integrated Biomarker Response" (IBR) described by Beliaeff and Burgeot (2002) was calculated. The procedure for IBR calculation of each biomarker response data is first standardized as Eq. (1):

$$Y_i = (X_i - m)/s \quad (1)$$

where Y_i is the standardized value of the biomarker, X_i is the mean value of a biomarker at each time point, and *m* and *s* are the mean value and standard deviation of a biomarker considering all the samples of different time points, respectively.

Then Z_i defined as the absolute value of Y_i was computed as $Z_i = Y_i$ or $Z_i = -Y_i$, in the case of a biomarker was activated or inhibited by contaminations, respectively, and the minimum value (min_i) for each biomarker at all time points was obtained and added to Z_i. After these, the score of each biomarker response (S_i) was calculated as:

$$S_i = Z_i + |min_i| \quad (2)$$

Finally, to achieve an integrated multi-biomarker response, star plots were used to display score results. The area A_i and corresponding IBR value were computed as:

$$A_i = \frac{S_i}{2} sin\alpha (S_i cos\beta + S_{i+1} sin\beta), \quad \beta = \arctan\left(\frac{S_{i+1}\sin\alpha}{S_i - S_{i+1}\cos\alpha}\right) \quad (3)$$

$$IBR = \sum_{i=1}^{n} A_i \quad (4)$$

where α is the angle between two adjacent lines, S_i and S_{i+1} represent two consecutive clockwise scores (radius coordinates) of the given star plot (Fig. 5).

2.7. Other analytical methods

The membrane integrity of biofilm was analyzed by LDH release assays (Hou et al., 2014). The LDH level was measured by a LDH kit (Jiancheng Bioengineering Co. Ltd., Nanjing, China) in accordance with the protocol specified by the manufacture. The biofilms with and without exposure were centrifuged at 12,000 × *g* for 5 min (Zheng et al., 2011). Then the supernatant was treated as instructed and measured at an absorption wavelength of 340 nm.

The bacteria viability in the fluvial biofilms with and without ZnO NPs treatments was examined via Live/Dead Biofilm Viability Kits. The viable bacteria were stained by SYTO® 9 (Ex/Em: 485/517 nm) and fluoresce green, while the damaged were stained by propidium iodide (Ex/Em: 536/617) and fluoresce red. The stained biofilms were observed using a confocal laser-scanning microscope (CLSM, Nikon A1, Japan). More details are provided in the Supplementary material.

All tests were performed in triplicate, and the results for each biomarker are presented as the mean ± standard deviation. Analyses of variance (ANOVA) performed with the SPSS software was used to evaluate the significant differences between treatments within each experiment ($p < 0.05$).

3. Results and discussion

3.1. ZnO NPs characterization

To observe the agglomeration behavior of ZnO NPs with different concentrations in exposure medium, the particles diameter and zeta potential were demonstrated in Table 1. After the suspensions still in room temperature for 24 h, a significant particle agglomeration was observed in 1 mg/L ZnO NPs in Milli-Q water, and the particle diameter increased to 152 ± 20 nm, much larger than the production description of 40–50 nm. Furthermore, the particle sizes of ZnO NPs in different concentrations of exposure

Table 1
Particles diameter and zeta potential of different concentrations of ZnO NPs suspensions in Milli-Q water and exposure medium after 24 h. Values are average ± standard deviation expressed (n=3).

ZnO-NPs suspensions (mg/L)	Particle sizes (nm)	Zeta potential (mV)
1 (in Milli-Q water)	152 ± 20	10.5 ± 1.22
1 (Exposure medium)	327 ± 16	11.3 ± 1.36
30 (Exposure medium)	1120 ± 21	10.3 ± 0.98
100 (Exposure medium)	1392 ± 37	12.8 ± 1.15

medium (1, 30 and 100 mg/L) reached to 327 ± 16, 1120 ± 21 and 1392 ± 37 nm, respectively. These results indicated that ZnO NPs tended to aggregate in suspension, and the particle diameters were influenced by the ions in nutrient solution due to compression of the electrical double layer (Kiser et al., 2010) as well as the concentrations of ZnO NPs. While previous studies have declared that the toxicity of NPs may be reduced due to the increasing size of NPs agglomeration (Choi and Hu, 2008).

Different from the increase in aggregate sizes, the zeta potential of ZnO NPs in the different test concentrations and medium showed a relatively stable values, about 11 mV, consistent with the findings of Miao et al. (2014) claiming that ZnO-NPs carried positive charges and zeta potential at pH < 8.

3.2. Adsorption of ZnO NPs onto biofilm and the toxicity effects on biofilm viability

Because of the wide structural diversity and numerous binding sites of biofilms, they have been widely applied both in wastewater treatment plants and natural waters (Guibaud et al., 2009; Mokaddem et al., 2009) to remove organic and inorganic contaminations. Besides, biosorption is believed to be the major mechanism for the pollutants removal and accompanied by the accumulation of the contaminations in the biofilms (Kiser et al., 2010). The SEM analysis has been widely employed in studies to investigate the adsorption of NPs to biofilms (Zheng et al., 2011; Hou et al., 2014). As seen in Fig. 1, a large number of ZnO NPs were adsorbed on the surface or in the matrixes of biofilms after 21 days exposure to 100 mg/L ZnO NPs, which was confirmed by the EDS examination of the biofilms. The same observations were also recorded in the researches exploring the potential effects of NPs on activated sludge or biofilms in wastewater treatment plants (Zheng et al., 2011; Hou et al., 2014). While studies have previously demonstrated that the adsorption of NPs onto biofilms or activated sludge could obviously reduce the bacteria viability and hence influence the wastewater treatment efficiency (Zheng et al., 2011; Hou et al., 2015b). Therefore, in this study, the CLSM technique was employed to further investigate the live and dead organisms in the exposed biofilm.

As seen from Fig. A.3 (Supplementary material), there is a quite spectacular contrast between the density of live and dead cells in the presence and absence of ZnO NPs. Nearly all of the microorganisms were dead after exposure to 100 mg/L ZnO NPs, suggesting that the viability of biofilm were highly decreased. Though some published studies on NPs ecotoxicity suggested several mechanisms/modes of action (Ma et al., 2013; Hou et al., 2015b), ROS were thought to be toxic by-products of biologically important oxygen metabolism (You et al., 2015). Furthermore, some types of NPs such as CuO and ZnO have been reported to cause the increase of LDH release and ROS production and thus affect the sludge membrane integrity and depress cell viability (Ma et al., 2013; Hou et al., 2015b).

As shown in Fig. 2, the elevation of ROS in 1 mg/L ZnO NPs was relative to the control, while in the high concentrations (30 and 100 mg/L) of exposure medium, the level of ROS reached to 184% and 244% of the control ($p < 0.05$). These findings indicated the occurrence of oxidative stress (Hou et al., 2015a) and the probable damage of function biomolecules in cells (such as DNA, protein and lipids) (George et al., 2009), which was in agreement with the increase of dead cells in Fig. A.3. However, the membrane integrity measurements confirmed that the presence of 1, 30 and 100 mg/L ZnO NPs induced no measureable LDH release than that of control. These results are consistent with those of Zheng et al. (2011) who acquired no considerable cell leakage in the activated sludge at the three concentrations of ZnO NPs. While considering the toxicity effects of ROS, the antioxidative systems of biofilms that were composed of different enzymatic and non-enzymatic mechanisms were expected to participate in the regulation of ROS levels to avoid the resulting stress damage (Collén et al., 2003; Valavanidis et al., 2006; Bonet et al., 2012). Among these enzymatic systems, SOD, CAT, GR and GSH-Px can transform peroxides into non-reactive species (Bonet et al., 2012, 2014), after both acute and chronic exposure to organic or inorganic pollutants (Valavanidis et al., 2006) and therefore were chosen in this study to test.

3.3. Response of the AEA to the toxicity effects of ZnO NPs

ROS is the generic terms of oxygen compounds including radical reactive oxygen forms (with odd electrons, i.e. $OH^{\cdot}$, $O_2^{\cdot -}$) and non-radical reactive oxygen forms (e.g. H_2O_2, $^1O_2$ and O_3) that readily engage in oxidation reactions and thus are potentially noxious to cells (Von Moos and Slaveykova, 2014). Among these forms, $OH^{\cdot}$ and $O_2^{\cdot -}$ are the most and second reactive, which results in the earliest responses of CAT and SOD aiming to estimate the superabundant $OH^{\cdot}$ and $O_2^{\cdot -}$ in cells, respectively (Bonet et al., 2012). As expected, the activity of CAT (Fig. 3a) was significantly induced ($p < 0.05$) at 0.25 day exposure, with all the concentrations of ZnO NPs treated. Similarly, the activity of SOD (Fig. 3b) was also remarkably increased at 0.25 day ($p < 0.05$), in the high concentrations of ZnO NPs exposure medium. The maximum SOD and CAT activities were observed at day 1 and 3 and correspond to an increase to 44.73 ± 6.18 and 53.51 ± 7.24 U/mg prot (compared with control of 14.88 ± 1.51 and 20.64 ± 4.51 U/mg prot), respectively, suggesting that the microorganisms were experiencing pollutant-induced superoxide radical stress (Cao et al., 2015). However, the gradual decreases of CAT and SOD activity were observed with incremental time and revealed an incomplete defense chain against occurrence of oxidative damage in organisms (Huang et al., 2007), which could be further confirmed by the increased density of dead cells in CLSM images.

As the first line defense against ROS (Cao et al., 2015), CAT and SOD destroys the free radical superoxide ($OH^{\cdot}$ and $O_2^{\cdot -}$) by converting them into peroxide and oxygen, namely H_2O_2, $^1O_2$ and O_3 (Jiang et al., 2015). Thus, as the second line of defense system, the activities of GR and GSH-Px, which have higher affinity in decomposing peroxide were measured to further explore the response of AEA to ZnO NPs exposure (Valavanidis et al., 2006). As shown in Fig. 4, both activities of GR and GSH-Px exhibited significant increase respect to the control at 3 days, which might be the results of the major generation of peroxide during this period (Jiang et al., 2015). The synergy between GR and GSH-Px can not only eliminate the peroxide effectively, but also activate the thiol enzyme in cells and thus protect the cytomembrane from ROS damage (Von Moos and Slaveykova, 2014), which may further explained the stable values of LDH in Fig. 2. Otherwise, the decrease in GR and GSH-Px activities with the prolonged exposure period might probably led to accumulation of peroxide and oxygen to toxic levels, ultimately inducing oxidative damage and organisms death (Jiang et al., 2015).

After long term exposure (21 days), the values of AEA in fluvial

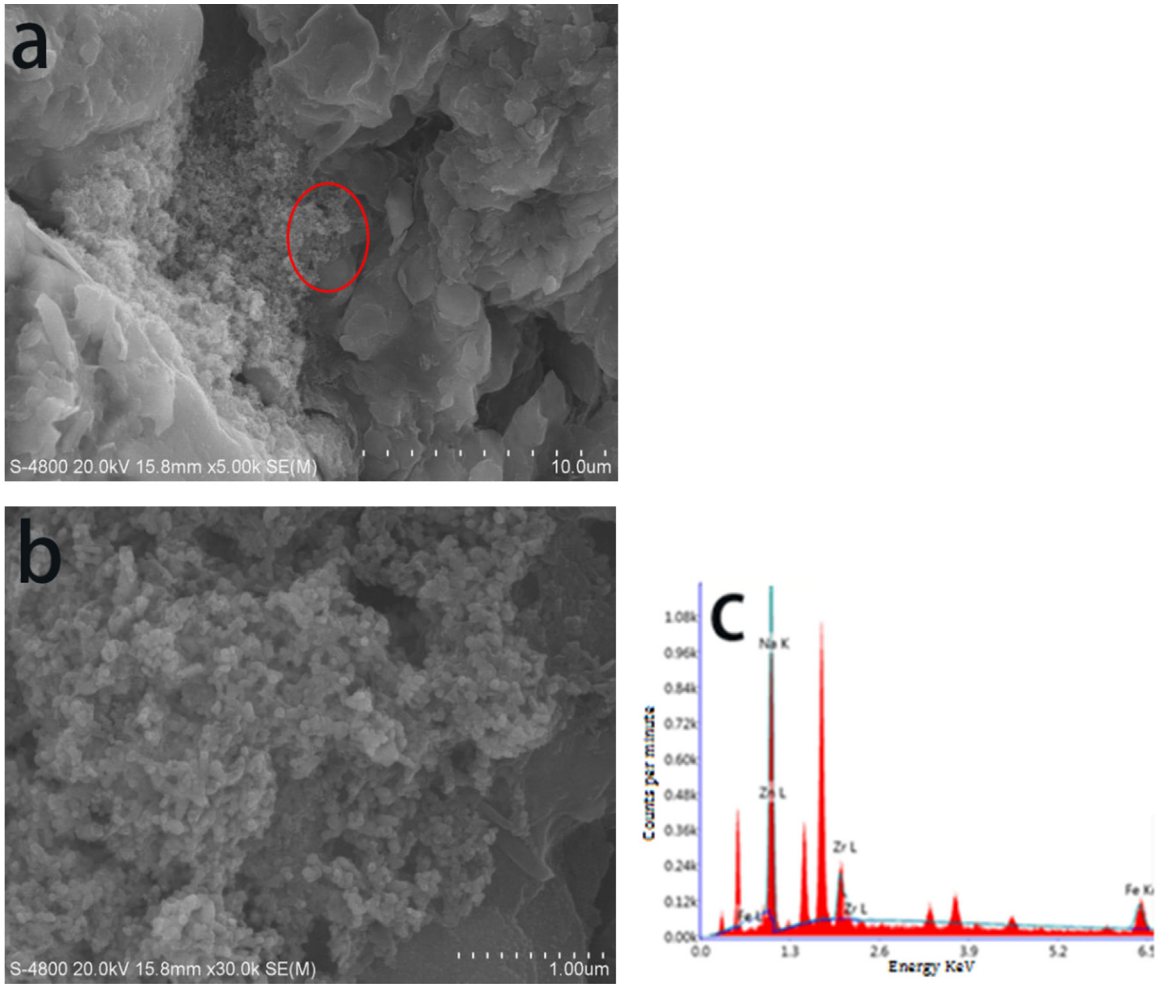

Fig. 1. SEM images of biofilm after biosorption for ZnO-NPs with concentration of 100 mg/L, (a) the biofilm surface under 10 μm; (b) the agglomeration of ZnO NPs on biofilm included in the red circle in (a) under 1 μm; (c) the energy dispersive spectrometer (EDS) of biofilm. (For interpretation of the references to color in this figure legend, the reader is referred to the web version of this article.)

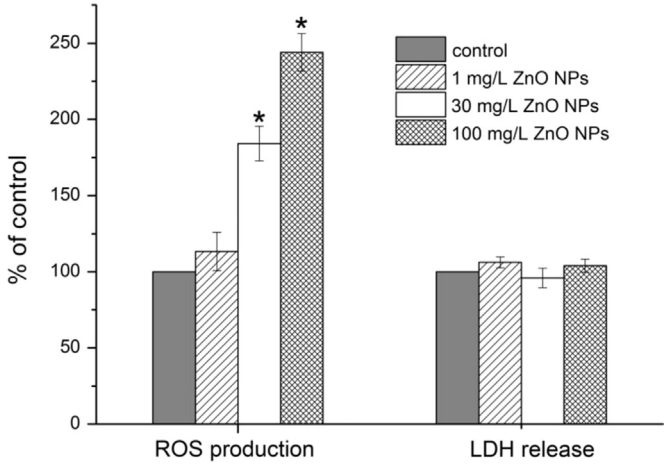

Fig. 2. Relative ROS production and LDH release in biofilms exposed to different concentrations of ZnO NPs. Error bars represent standard deviations of triplicate measurements. Asterisks indicate statistical differences ($p < 0.05$) from the control.

biofilms exposed to 1 mg/L ZnO NPs were comparable to the control, confirming the no obvious changes in ROS generation and microorganisms viability in Figs. 2 and A.3. While exposure to 30 and 100 mg/L ZnO NPs, all the enzymes tested in this study followed a similar fluctuating trend of being activated in the initial 3 days and inhibited at the end of exposure, suggesting that the biological response of biofilms to ZnO NPs exposure existed as well as obvious adaptative threshold. Furthermore, the measureable decreased activities of CAT, GR and GSH-Px after exposure to 100 mg/L ZnO NPs declared an overwhelming of the antioxidant defenses (Bonnineau, 2011), which was reported to be caused by the abundance of dissolved Zn^{2+} from ZnO NPs in our previous study (Xu et al., 2016). Particularly, SOD activity showed a significant activation after exposure to 30 and 100 mg/L ZnO NPs for 21 days, which might mainly attributed to its location in cells or the presence of Zn-SOD isoform in cytosol (Allen and Tresini, 2000) and need to be further investigated. The GR content showed a more obvious manner dependent on different concentrations of ZnO NPs, which may ascribed to the different operating rate of glutathione/ascorbate cycle with different concentrations of NPs exposure (Jiang et al., 2015).

It is important to point out that the CAT and SOD activities are the first functional endpoints, showing much earlier responses to 30 mg/L ZnO NPs exposure after 0.25 day than photosynthetic parameters after 3 days in our previous study (Xu et al., 2016). In addition, the AEA in fluvial biofilms could be induced by 1 mg/L ZnO NPs exposure after 0.25, 1 and 3 days, more sensitive than photosynthetic parameters and community composition showing measureable difference with control after 7 days (Xu et al., 2016). Additionally, Guasch et al. (2010) also declared that in freshwater biofilms, AEA were proved to be more sensitive to Cu exposure than photosynthetic parameters. The role of AEA in scavenging

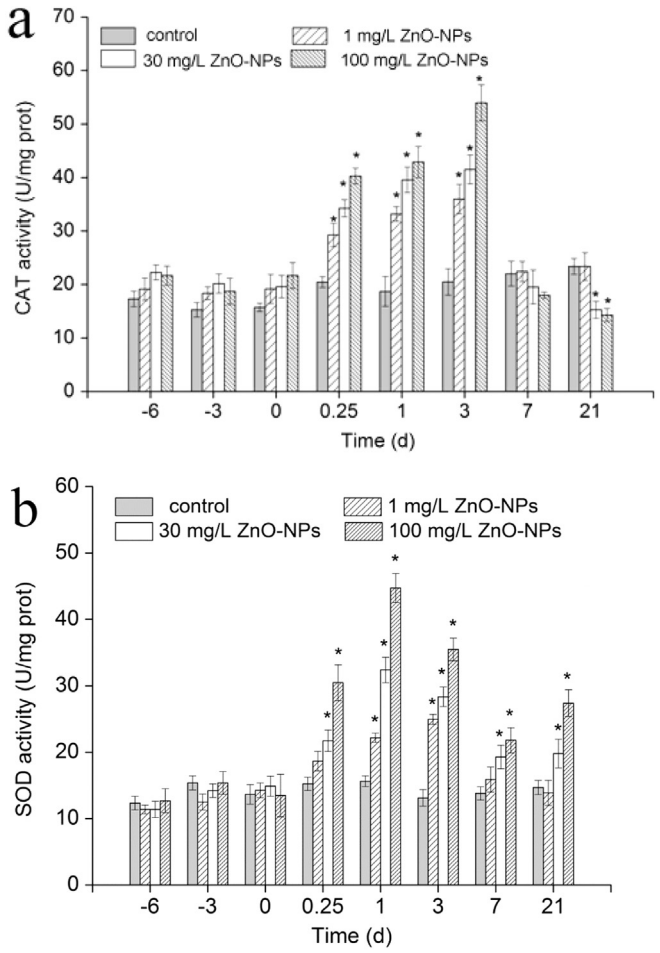

Fig. 3. Changes of CAT (a) and SOD (b) activities in biofilms with ZnO-NPs treatment over time and concentrations. Error bars represent standard deviations of triplicate measurements. Asterisks indicate statistical differences ($p < 0.05$) from the control.

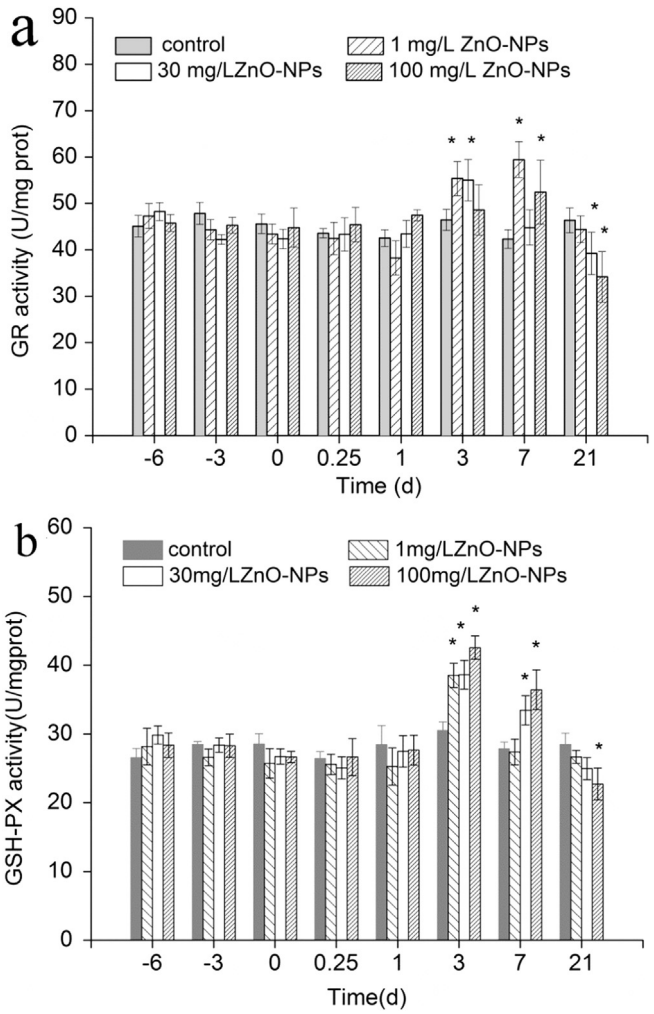

Fig. 4. Changes of GR (a) and GSH-Px (b) activities in biofilms with ZnO-NPs treatment over time and concentrations. Error bars represent standard deviations of triplicate measurements. Asterisks indicate statistical differences ($p < 0.05$) from the control.

ROS with fast and sensitive responses was expected to convert the free radical superoxide to peroxide and finally decompose peroxide into non-toxic forms (Von Moos and Slaveykova, 2014). Without the antioxidants, ROS will directly or indirectly via the products of lipid peroxidation, cause indiscriminate damage to cellular components including nucleic acid, enzymes and membranes (Ševců et al., 2011). We thus highlighted the interest of AEA in fluvial biofilms as sensitive biomarkers of ZnO NPs ecotoxicity.

3.4. Integrated assessment of AEA response values

The IBR index, which scores and summarizes the responses of multiple biomarkers into a single value, provides an intuitive interpretation of the health status of the organisms (Kim et al., 2010). Through integrating the AEA and their weighting (Fig. 5a-d), the IBR values were computed (Fig. 5e). With 1 and 30 mg/L ZnO NPs exposure, the value of IBR at 3 days was highlighted, associated to the responses of GR and GSH-Px (Fig. 5c and d), probably resulting from the excessive production of non-radical peroxide at this period (Jiang et al., 2015). However, the IBR value of the biofilms exposed to 100 mg/L ZnO NPs showed a maximum level at 0.25 day, which was related to the responses of CAT and SOD (Fig. 5a and b) and impacted by the production of radical superoxide (Von Moos and Slaveykova., 2014). Additionally, since higher IBR values manifest the increased biological responses and poorer health condition of the biofilms (Brooks et al., 2015), the calculated IBR values (Fig. 5e) in the present study also displayed a distinct toxic and temporal variation (Suman et al., 2015) that the higher concentrations of ZnO NPs exposure posed the stronger toxicity effects in a shorter time. The recovery ability of biofilms to high concentrations of ZnO NPs (30 and 100 mg/L) should be considered after 3 and 0.25 days (Fig. 5e). While the IBR level of 1.26 indicated the adaptive responses to oxidative stress (Fig. 2) caused by 1 mg/L ZnO NPs. Moreover, through analyzing the weighting of standardized biomarker responses in IBR values, the higher toxicity effects of radical reactive oxygen forms (i.e. $OH^{\cdot}$, $O_2^{\cdot -}$) than non-radical reactive oxygen forms (e.g. H_2O_2, $^1O_2$ and O_3) (Von Moos and Slaveykova., 2014) could also be confirmed. These observations were consistent with the researches using IBR approach with other organisms, including mussels (Brooks et al., 2015) and fish (Kim et al., 2010; Li et al., 2011; Suman et al., 2015), which also emphasized the potential use of IBR as an integrated interpretation of biological effects of contaminants.

Through integrating the responses of four antioxidant enzymes into a signal value, the general toxicity process of different concentrations of ZnO NPs as well as the health status of biofilms were obtained and the results were consistent with Figs. 2 and A.3. These results indicated that IBR can be a practical tool for the assessment of toxicity effects and ecological risk of ZnO NPs. IBR is an oversimplification of biomarkers and maybe the tendency of IBR values between two time points is not accurately linear, since

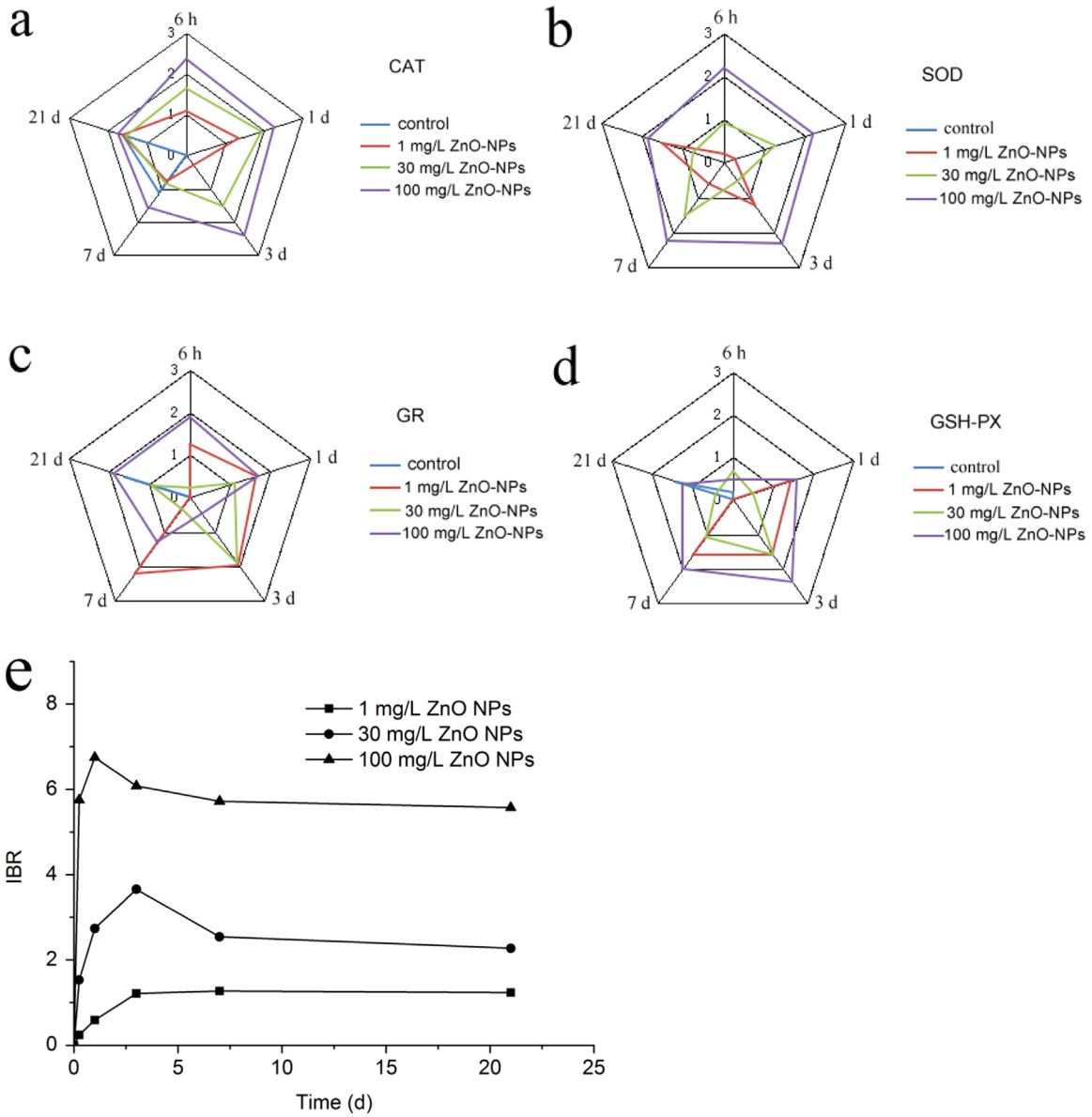

Fig. 5. Star plots of standardized biomarker responses of AEA (a-d) and IBR values (e) of biofilm during the exposure.

Broeg and Lehtonen (2006) highlighted that the IBR result should not be taken at "face value" but rather as a tool to direct further actions.

4. Conclusions

Antioxidant enzyme activities as biomarkers of fluvial biofilm to ZnO NPs toxicity and the Integrated Biomarker Responses (IBR) assessment were studied.

The biosorption of high concentrations of ZnO NPs as aggregates induced the substantial losses of microorganisms in biofilm and the measurable ROS production further explained the potential mechanisms, though the values of LDH remained unchanged after the exposures.

AEA played a key role in coping with ROS and protecting the biofilm from damage, though were inhibited after long term exposure to ZnO NPs. Additionally, the fast responses (0.25 day) of AEA to 1 mg/L of ZnO NPs exposure supported its application as an early warner of toxicity exposure. This information can be interesting for enhancing current tools used for risk assessment, providing the basis to evaluate the functional effects of ZnO NPs toxicity in real exposure scenarios.

Overall, the IBR levels showed an integrated view on biological effects of ZnO NPs and may be useful for assessing the health condition of fluvial biofilms with temporal variations of ZnO NPs exposure. Thus the IBR may be used as a constructive method to evaluate the toxicity effects and ecological risk of ZnO NPs toward biofilms.

Acknowledgments

We are grateful for the grants from the project supported by the National Science Funds for Creative Research Groups of China (No. 51421006), the National Natural Science Foundation of China (Nos. 51479047, 51479065, and 51209069), the National Science Funds for Distinguished Young Scholars (No. 51225901), the Program for Changjiang Scholars and Innovative Research Team in University (No. IRT13061), the Key Program of National Natural Science Foundation of China (No. 41430751), the Chinese

Universities Scientific Fund (No. 2015B05714) and PAPD.

Appendix A. Supplementary material

Supplementary data associated with this article can be found in the online version at doi:10.1016/j.ecoenv.2016.06.014.

References

Aebi, H., 1984. Catalase in vitro. Methods Enzym. 105, 121.

Adams, L.K., Lyon, D.Y., Alvarez, P.J.J., 2006. Comparative ecotoxicity of nanoscale TiO_2, SiO_2, and ZnO water suspensions. Water Res. 40, 3527–3532.

Allen, R.G., Tresini, M., 2000. Oxidative stress and gene regulation. Free Radic. Biol. Med. 28, 463–499.

Battin, T.J., Kaplan, L.A., Newbold, J.D., Hansen, C.M., 2003. Contributions of microbial biofilms to ecosystem processes in stream mesocosms. Nature 426, 439–442.

Beliaeff, B., Burgeot, T., 2002. Integrated biomarker response: a useful tool for ecological risk assessment. Environ. Toxicol. Chem. 21, 1316–1322.

Bonet, B., Corcoll, N., Guasch, H., 2012. Antioxidant enzyme activities as biomarkers of Zn pollution in fluvial biofilms. Ecotoxicol. Environ. Saf. 80, 172–178.

Bonet, B., Corcoll, N., Tlili, A., Morin, S., Guasch, H., 2014. Antioxidant enzyme activities in biofilms as biomarker of Zn pollution in a natural system: an active bio-monitoring study. Ecotoxicol. Environ. Saf. 103, 82–90.

Bonnineau, B., 2011. Contribution of Antioxidant Enzymes to Toxicity Assessment in Fluvial Biofilms (Masters Thesis). University of Girona, Catalonia, Spain.

Boxall, A.B., Chaudhry, Q., Sinclair, C., Jones, A., Aitken, R., Jefferson, B., Watts, C., 2007. Current and Future Predicted Environmental Exposure to Engineered Nanoparticles. Central Science Laboratory, Department of the Environment and Rural Affairs, London, UK, p. 89.

Brar, S.K., Verma, M., Tyagi, R.D., Surampalli, R.Y., 2010. Engineered nanoparticles in wastewater and wastewater sludge – evidence and impacts. Waste Manag. 30, 504–520.

Broeg, K., Lehtonen, K.K., 2006. Indices for the assessment of environmental pollution of the Baltic Sea coasts: integrated assessment of a multi-biomarker approach. Mar. Pollut. Bull. 53, 508–522.

Brooks, S.J., Harman, C., Hultman, M.T., Berge, J.A., 2015. Integrated biomarker assessment of the effects of tailing discharges from an iron ore mine using blue mussels (Mytilus spp.). Sci. Total Environ. 524, 104–114.

Cao, D.J., Shi, X.D., Li, H., Xie, P.P., Zhang, H.M., Deng, J.W., Liang, Y.G., 2015. Effects of lead on tolerance, bioaccumulation, and antioxidative defense system of green algae, Cladophora. Ecotoxicol. Environ. Saf. 112, 231–237.

Choi, O., Hu, Z., 2008. Size dependent and reactive oxygen species related nanosilver toxicity to nitrifying bacteria. Environ. Sci. Technol. 42, 4583–4588.

Clements, W.H., Newman, M.C., 2002. Community Ecotoxicology. John Wiley & Sons, Ltd., West Sussex, UK, p. 336.

Collén, J., Pinto, E., Pedersen, M., Colepicolo, P., 2003. Induction of oxidative stress in the red macroalga *Gracilaria tenuistipitata* by pollutant metals. Arch. Environ. Contam. Toxicol. 45, 337–342.

Cuypers, A., Vangronsveld, J., Clijsters, H., 2001. The redox status of plant cells (AsA and GSH) is sensitive to zinc imposed oxidative stress in roots and primary leaves of *Phaseolus vulgaris*. Plant Physiol. Biochem. 39, 657–664.

Flemming, H.C., Wingender, J., 2010. The biofilm matrix. Nat. Rev. Microbiol. 8, 623–633.

George, S., Pokhrel, S., Xia, T., Gilbert, B., Ji, Z., Schowalter, M., Rosenauer, A., Damoiseaux, R., Bradley, K., Madler, L., Nel, A.E., 2009. Use of a rapid cytotoxicity screening approach to engineer a safer zinc oxide nanoparticle through iron doping. ACS Nano 4, 15–29.

Guasch, H., Atli, G., Bonet, B., Corcoll, N., Leira, M., Serra, A., 2010. Discharge and the response of biofilms to metal exposure in Mediterranean rivers. Hydrobiologia 657, 143–157.

Guibaud, G., van Hullebusch, E., Bordas, F., d'Abzac, P., Joussein, E., 2009. Sorption of Cd (II) and Pb (II) by exopolymeric substances (EPS) extracted from activated sludges and pure bacterial strains: modeling of the metal/ligand ratio effect and role of the mineral fraction. Bioresour. Technol. 100, 2959–2968.

Hendren, C.O., Mesnard, X., Dröge, J., Wiesner, M.R., 2011. Estimating production data for five engineered nanomaterials as a basis for exposure assessment. Environ. Sci. Technol. 45, 2562–2569.

Hou, J., Miao, L., Wang, C., Wang, P., Ao, Y., Qian, J., Dai, S., 2014. Inhibitory effects of ZnO nanoparticles on aerobic wastewater biofilms from oxygen concentration profiles determined by microelectrodes. J. Hazard. Mater. 276, 164–170.

Hou, J., Miao, L., Wang, C., Wang, P., Ao, Y., Lv, B., 2015a. Effect of CuO nanoparticles on the production and composition of extracellular polymeric substances and physicochemical stability of activated sludge flocs. Bioresour. Technol. 176, 65–70.

Hou, J., You, G., Xu, Y., Wang, C., Wang, P., Miao, L., Ao, Y., Li, Y., Lv, B., 2015b. Effects of CeO_2 nanoparticles on biological nitrogen removal in a sequencing batch biofilm reactor and mechanism of toxicity. Bioresour. Technol. 191, 73–78.

Hua, X., Li, M., Su, Y., Dong, D., Guo, Z., Liang, D., 2012. The degradation of linear alkylbenzene sulfonate (LAS) in the presence of light and natural biofilms: the important role of photosynthesis. J. Hazard. Mater. 229, 450–454.

Huang, D.J., Zhang, Y.M., Song, G., Long, J., Liu, J.H., Ji, W.H., 2007. Contaminants-induced oxidative damage on the carp Cyprinus carpio collected from the upper Yellow River, China. Environ. Monit. Assess. 128, 483–488.

Jiang, J., Qin, C., Shu, X., Chen, R., Song, H., Li, Q., Xu, H., 2015. Effects of copper on induction of thiol-compounds and antioxidant enzymes by the fruiting body of *Oudemansiella radicata*. Ecotoxicol. Environ. Saf. 111, 60–65.

Kim, W.K., Lee, S.K., Jung, J., 2010. Integrated assessment of biomarker responses in common carp (*Cyprinus carpio*) exposed to perfluorinated organic compounds. J. Hazard. Mater. 180, 395–400.

Kiser, M.A., Ryu, H., Jang, H., Hristovski, K., Westerhoff, P., 2010. Biosorption of nanoparticles to heterotrophic wastewater biomass. Water Res. 44, 4105–4114.

Lars, H., Johansson, L.H., Borg, L.A.H., 1988. A spectrophotometric method for determination of catalase activity in small tissue samples. Anal. Biochem. 174, 331–336.

Le Faucheur, S., Behra, R., Sigg, L., 2005. Phytochelatin induction, cadmium accumulation, and algal sensitivity to free cadmium ion in *Scenedesmus vacuolatus*. Environ. Toxicol. Chem. 24, 1731–1737.

Li, X.Y., Yang, S.F., 2007. Influence of loosely bound extracellular polymeric substances (EPS) on the flocculation, sedimentation and dewaterability of activated sludge. Water Res. 41, 1022–1030.

Li, Z.H., Velisek, J., Zlabek, V., Grabic, R., Machova, J., Kolarova, J., Li, P., Randak, T., 2011. Chronic toxicity of verapamil on juvenile rainbow trout (*Oncorhynchus mykiss*): effects on morphological indices, hematological parameters and antioxidant responses. J. Hazard. Mater. 185, 870–880.

Limbach, L.K., Wick, P., Manser, P., Grass, R.N., Bruinink, A., Stark, W.J., 2007. Exposure of engineered nanoparticles to human lung epithelial cells: influence of chemical composition and catalytic activity on oxidative stress. Environ. Sci. Technol. 41, 4158–4163.

Ma, H., Williams, P.L., Diamond, S.A., 2013. Ecotoxicity of manufactured ZnO nanoparticles – a review. Environ. Pollut. 172, 76–85.

Maynard, A.D., Aitken, R.J., Butz, T., Colvin, V., Donaldson, K., Oberdörster, G., Philbert, M.A., Ryan, J., Seaton, A., Stone, V., Tinkle, S.S., Tran, L., Walker, N.J., Warheit, D.B., 2006. Safe handling of nanotechnology. Nature 444, 267–269.

Miao, L.Z., Wang, C., Hou, J., Wang, P.F., Qian, J., Dai, S.S., 2014. Kinetics and equilibrium biosorption of nano-ZnO particles on periphytic biofilm under different environmental conditions. J. Environ. Inform. 23, 1–9.

Mohandas, J., Marshall, J.J., Duggin, G.G., Horvath, J.S., Tiller, D.J., 1984. Differential distribution of glutathione and glutathione-related enzymes in rabbit kidney: possible implications in analgesic nephropathy. Biochem. Pharmacol. 33, 1801–1807.

Mokaddem, H., Sadaoui, Z., Boukhelata, N., Azouaou, N., Kaci, Y., 2009. Removal of Cadmium from aqueous solution by polysaccharide produced from *Paenibacillus polymyxa*. J. Hazard. Mater. 172, 1150–1155.

Nowack, B., Bucheli, T.D., 2007. Occurrence, behavior and effects of nanoparticles in the environment. Environ. Pollut. 150, 5–22.

Park, E.J., Choi, J., Park, Y.K., Park, K., 2008. Oxidative stress induced by cerium oxide nanoparticles in cultured BEAS-2B cells. Toxicology 245, 90–100.

Roco, M.C., 2005. The emergence and policy implications of converging new technologies integrated from the nanoscale. J. Nanopart. Res. 7, 129–143.

Serda, R.E., Ferrati, S., Godin, B., Tasciotti, E., Liu, X., Ferrari, M., 2009. Mitotic trafficking of silicon microparticles. Nanoscale 1, 250–259.

Serafim, A., Company, R., Lopes, B., Fonsec, V.F., Franca, S., Vasconcelos, R.P., Bebianno, M.J., Cabral, H.N., 2012. Application of an integrated biomarker response index (IBR) to assess temporal variation of environmental quality in two Portuguese aquatic systems. Ecol. Indic. 19, 215–225.

Ševců, A., El-Temsah, Y.S., Joner, E.J., Černík, M., 2011. Oxidative stress induced in microorganisms by zero-valent iron nanoparticles. Microbes Environ. 26, 271–281.

Suman, T.Y., Rajasree, S.R., Kirubagaran, R., 2015. Evaluation of zinc oxide nanoparticles toxicity on marine algae chlorella vulgaris through flow cytometric, cytotoxicity and oxidative stress analysis. Ecotoxicol. Environ. Saf. 113, 23–30.

Tripathi, B.N., Mehta, S.K., Amar, A., Gaur, J.P., 2006. Oxidative stress in Scenedesmus sp. during short-and long-term exposure to Cu^{2+} and Zn^{2+}. Chemosphere 62, 538–544.

Valavanidis, A., Vlahogianni, T., Dassenakis, M., Scoullos, M., 2006. Molecular biomarkers of oxidative stress in aquatic organisms in relation to toxic environmental pollutants. Ecotoxicol. Environ. Saf. 64, 178–189.

Von Moos, N., Slaveykova, V.I., 2014. Oxidative stress induced by inorganic nanoparticles in bacteria and aquatic microalgae – state of the art and knowledge gaps. Nanotoxicology 8, 605–630.

Wang, Z.L., Song, J., 2006. Piezoelectric nanogenerators based on zinc oxide nanowire arrays. Science 312, 242–246.

Xu, Y., Wang, C., Hou, J., Dai, S., Wang, P., Miao, L., Lv, B., Yang, Y., You, G., 2016. Effects of ZnO nanoparticles and Zn^{2+} on fluvial biofilms and the related toxicity mechanisms. Sci. Total Environ. 544, 230–237.

You, G., Hou, J., Xu, Y., Wang, C., Wang, P., Miao, L., Ao, Y., Li, Y., Lv, B., 2015. Effects of CeO_2 nanoparticles on production and physicochemical characteristics of extracellular polymeric substances in biofilms in sequencing batch biofilm reactor. Bioresour. Technol. 194, 91–98.

Zheng, X., Wu, R., Chen, Y., 2011. Effects of ZnO nanoparticles on wastewater biological nitrogen and phosphorus removal. Environ. Sci. Technol. 45, 2826–2832.

Zhu, X., Yuri, I., Gan, X., Suzuki, I., Li, G., 2007. Electrochemical study of the effect of nano-zinc oxide on microperoxidase and its application to more sensitive hydrogen peroxide biosensor preparation. Biosens. Bioelectron. 22, 1600–1604.